The Tungsten Oxide Within Phosphate Glasses to Investigate the Structural, Optical and Shielding Properties Variations

mohammed sadeq (mhmd_sa3d@hotmail.com)
Sinai university https://orcid.org/0000-0003-1457-0269
B.O. El-bashir
University of Tabouk: University of Tabuk
Aljawhara H. Almuqrin
Umm Al-Qura University
M.I. Sayyed
Isra University

Research Article

Keywords: Phosphate glassed, WO3, Radiation shielding

Posted Date: February 23rd, 2021

DOI: https://doi.org/10.21203/rs.3.rs-225346/v1

Version of Record: A version of this preprint was published at Journal of Materials Science: Materials in Electronics on April 15th, 2021. See the published version at https://doi.org/10.1007/s10854-021-05871-0.

The tungsten oxide within phosphate glasses to investigate the structural, optical and shielding properties variations

M.S. Sadeq[1,*], B.O. El-bashir[2,3], Aljawhara H. Almuqrin[4], M.I. Sayyed[5,6]

[1] Basic Sciences Department, Faculty of Engineering, Sinai University, Al-Arish, Egypt.

[2]Department of physics, Faculty of Science, University of Tabuk, Tabuk, Saudi Arabia

[3]Institute of Laser, Sudan University of Science and Technology (SUST), Sudan

[4] Department of physics, college of science, Princess Nourah bint Abdulrahman University, Riyadh, Saudi Arabia.

[5] Department of Physics, Faculty of Science, Isra University, Amman, Jordan.

[6] Department of Nuclear Medicine Research, Institute for Research and Medical Consultations (IRMC), Imam Abdulrahman bin Faisal University (IAU), P.O. Box 1982, Dammam,31441, Saudi Arabia.

Keywords: Phosphate glassed; WO_3, Radiation shielding

[*]Corresponding author: mhmd_sa3d@hotmail.com

Abstract

We prepared a series of sodium phosphate glasses by changing WO_3/P_2O_5 content and investigated structure optical and radiation shielding features as a function of glass composition. The average density (ρ_{exp}) and was found to increase gradually from 2.49 to 3.07 g/cm^3 while the average molar volume values reduced from 47.37 to 44.28 cm^3/mol with WO_3 addition. Also, the average field strength was also computed and found to increase with increasing WO_3. The study of optical absorption spectra reveals that, the absorption peaks in the visible region become higher compared to the peaks In the UV region. This observation is accompanied with a color transformation of

glasses from light to dark blue color, with more WO_3 adding. The existence of pentavalent tungsten state (W^{5+}) is identified by this blue color. with WO_3 addition an absorption band at around at 350–390 nm is appeared. Moreover, this band is overlapped with Urbach edge, which regularly produces an artificial edge-like feature at ~400 nm. A detailed deconvolution protocol is required for an appropriate understanding of these spectra and unravelling the hidden Urbach edge. Our analysis shows that, with increasing WO_3/P_2O_5 content, the optical band gap decreases. This behavior can be elucidated in terms of lower band gap of W (2.7 eV) than that of P_2O_5 (8.5 eV) and the high polarizing power W. Further, the radiation shielding parameters were investigated for the prepared glasses. WO_3 addition improves these shielding parameters against radiation. Where, upon the increase of WO_3 concentration, the LAC of glass material increases which leads to a decrease in HVL value. Then it is deducible that the amount of WO_3 in this glass sample has an important impact on the shielding capability at lower energy values and has a slight impact at higher energy values.

1. Introduction

The fabrication of novel glass compositions is a very dynamic field of research due to their motivating applications in our daily life, and the capability of fabrication and flexibility of shape and size at quite low cost [1]. A conventional glassy matrix former for example silicate (SiO_4-based), borate (B_2O_3-based), and phosphate (P_2O_5-based) with varied formulas of modifiers and intermediates were studied for numerous technological appliances. From literature it is well-known that, P_2O_5-based glasses with their excellent thermal properties (low melting temperature and high

thermal expansion coefficient) are promising sealing materials [1], excellent UV–VIS transparent windows and a wide range of solubility for glass modifiers for example alkali, rare earth (RE) and transition metals [2], appropriate candidates for lenses fabrication that diminish color distortion and acceptable in numerous optical applications [3-5], and appropriate candidates for optical memories and optical data storage [6,7]. The structure of P_2O_5-based glasses deeply relies on type and quantity of glass modifier in the glassy matrix. Thus, the glassy state of $NaPO_3$ or P_2O_5 glass formers can transform from Q^3 sets, containing three bridging oxygens (BO), to Q^2, Q^1 and Q^0 sets with two, three and four non-bridging oxygens (NBO), respectively [1].

From literature it is well-known that, transition metal cations as dopants in glasses can change the mechanisms and processes for the creation of radiation induced color centers, depending on the type and concentration of transition metal cations as well as the formulation of host glass [8]. The existence of W^{5+} cations may create $W^{5+}O_3$ molecular orbital states and possibly help in the depolymerization of the glassy matrix by break into P-O-P links. Moreover, the insertion of WO_3 in phosphate glasses within high amounts (>10 mol%) reduces the maximum phonon energy of the phosphate matrix by development of highly polarizable WO_6 clusters, resulting interesting features such as photochromism and nonlinear optical absorption [9]. The addition of WO_3 is well-known to enhance mechanical, chemical and thermal stabilities [10]. Previous investigations on WO_3-containing phosphate glasses [3,8] have reported that, these glasses show bluish color and various characteristic optical absorption bands representing to the existence of W^{5+} (pentavalent) cations.

Further, the usage of shielding glasses in radiation protection applications is increasing day after day. Because of their motivating characteristics such as excellent transparency, capability of fabrication, low fabrication cost, and good thermal and structural features. Along with that, the radiation shielding parameters of glass systems can be altered by using different contents of oxides in the glass formula [11-14]. Tungsten oxide were found to increase shielding performance of oxide glasses against gamma irradiation [15,16].

In this Article, we prepared WO_3-doped tungsten phosphate glasses, characterize them to study the microstructural–properties relationships, in view of their structure, optical and radiation shielding applications.

2. Experiment Section

Studied ternary sodium phosphate glasses with the formula [30 mol% Na_2O - (70-Y) mol% P_2O_5 - Y mol% WO_3], (Y=0, 5, 10, 15 and 20 mol %), synthesized using melt quenching method, where analytical grade sodium dihydrogen orthophosphate, tungsten oxide and sodium oxide supplied by Sigma Aldrich Co. Precalculated weights of chemicals needed for glass fabrication in mol percent were put in a 50 ml porcelain container in a an electric furnace regulated at about 1100 °C for 90 minutes to assure homogenous and bubble free melts.

Density data calculated from the Archimedean principle by obtaining the weight of each specimen before and after immersion in stable liquid as xylene. Measurements of specimens repeated four times (N=4) to obtain the error in the average density and average molar volume. The error in the average density is calculated from the formula

$$\rho_{exp} = \frac{\sum \rho_{exp}}{N} \pm \frac{\rho_{max} - \rho_{min}}{2\sqrt{N}} \quad (1)$$

and the uncertainty in the average molar volume is

$$V_{exp} = \frac{\sum V_{exp}}{N} \pm \frac{2\sqrt{N} * \rho^2 * M}{\rho_{max} - \rho_{min}} \quad (2)$$

Absorbance (A) of all glass specimens was performed using a double beam spectrophotometer, model JASCO within 200 to 1100 nm.

3. Results and Discussion

3.1 Optical Properties

3.1.1 The nature of the W^{3+}, W^{4+}, W^{5+} and W^{6+} states and color of phosphate glasses (origin of blue color)

The study of optical absorption spectrum is a suitable method to give information regarding the optical transitions in glass. Besides, this study provides information for the electronic band structure in glassy material. The absorbance spectra of NaPW-glasses were considered in wavelength region (300–1050 nm) and are presented in Fig. 1(a). It was notice from Fig. 1(a) that, with increasing WO_3 in glasses the absorption peaks in the visible region become higher compared to the peaks In the UV region. This observation is accompanied with a color transformation of NaPW-glasses from light blue color to dark blue, with more WO_3 adding. The existence of pentavalent tungsten state (W^{5+}) is identified experimentally from producing a distinct bluish color in the glass [17]. In order to discuss this color

transformation, and the absorption peaks in the visible region the succeeding arguments are considered [3,7–9,18,21]:

I. it is well-known, W cations have four oxidation states; triv-(W^{3+}), tetra-(W^{4+}), penta-(W^{5+}), and hexavalent -(W^{6+}), while the amount of each state is dependent on kind and composition of glass in addition to melting circumstances. As well it is supposed that WO_3 can developed definite structural units inside the glassy matrix such as $WO_{4(td)}$ and $WO_{6(oct)}$ of W^{6+} cations and $(W^{5+}\ O_3)_{(oct)}$ of W^{5+} cations.

II. The existence of pentavalent tungsten state (W^{6+}) is recognized by experimentation from producing UV band at around 360–390 nm due to the charge transfer, moreover, W^{6+} is an exceptional arrangement that represent the d° configuration demonstrating paired electrons. The remainder of the tungsten valences (+3, +4, +5) are identified to reveal characteristic visible bands [3,7–9,18,21].

III. Moncke and Ehrt [20,21] reported the consistent absorption bands for the three lower valences of W cations. The D-d bands at 350 and 440 nm are associated to (W^{3+}, d^3), (W^{4+}, d^2) display visible bands at about 455, 555, 655 nm and the (W^{5+}, d^1) display a very broad band positioned at around 785 nm.

For deep analyses for optical spectra a detailed deconvolution protocol is required. The deconvolution of these spectra and the related details shows visible bands positioned at about 380-420, 580–600 nm and 830–860 nm as shown in Figure 1b. These latter three broad bands signify to the existence of (W^{3+}, d^3), (W^{4+}, d^2) and (W^{5+}, d^1), respectively. Also, the optical spectra display that, the heights of the broad bands referring to W^{3+}, W^{4+} and W^{5+} increase compared to W^{6+} with further WO_3 doping.

Similar results were previously reported for sodium metaphosphate glass [3] and cadmium zinc phosphate glasses doped with WO_3 [22]. This increment in intensities is accompanied by a red shift towards the longer wavelength with further WO_3 doping. This shift towards the longer wavelength might be attributed to the increment in the average bond length of W-O with the regular increase of WO_3 from 5 to 20 mol%. The increase in the absorption band intensities (in the visible region) with further WO_3 doping is in an excellent consistence with Beer–Lambert–Bouguer's Law [23,24]. Furthermore, such increase in the absorption bands is the reason for color transformation of NaPW-glasses from light to dark blue color.

3.1.2 The UV absorption bands and optical band gap

The investigation of optical absorption in the UV range is a suitable tool to recognize the band structures of electrons in glasses. In these optical spectra of glasses, a fast increase in the absorbance toward smaller wavelengths (□) is observed. The fast increase of absorption coefficient (α) is described as the fundamental absorption edge (UV "cut off"). Further than this UV "cutoff", glasses is opaque for electromagnetic radiation. Where the photon energy larger than the optical band gap (i.e. □≤ 200 nm) that presents between the valence and conduction bands. In glasses, estimating this band gap can give information about structural modifications and the chemical bonds inside the glass network. In addition to, determining semiconducting features of materials used for opto-electronic and photocatalyst devices. The width of the localized states in the band gap which created as a result to the disorder inside the material can

also be estimated from the study of the optical absorption spectrum for such material [25].

Essentially, two forms of transitions can happen near the fundamental absorption edge of both crystalline and amadelphous materials – direct and indirect transitions. In the case of indirect transition, simultaneous interactions among the electron and lattice vibrations (phonons) are happened. In this case, the electron's wave vector can be changed due to the phonon's absorption/emission. Further, for indirect transition, the lowest point of the conduction band and the highest point of the valence band lie in a dissimilar k-space. On the other hand, for the direct optical transitions, it is necessary for the wave vector of an electron to be the same as it absorbs a photon [26,27].

For the present glasses, in the ultraviolet region, one can observe a strong UV absorption band (at 300 nm) are ascribed to the charge transfer mechanism. Consequently, the strong UV absorption band displayed in Figure 1a for the W free sample is attributed to the presence of ferric cations traces (Fe^{3+}) as impurities inside the chemicals intended for the preparation process of the NaPW-glasses. With further WO_3 doping, UV absorption bands at 350–390 nm. This confirms the existence of all the tungsten cations in their W^{6+} state. Moreover, this band is overlapped with the fundamental absorption edge (UV "cut off"), which regularly produces an artificial edge-like. This overlapping is observed as broadening in the UV band (marked * in Figure 1a). A detailed deconvolution protocol is required to overcome this overlapping and extract appropriate details (to unravelling the hidden absorption edge). Figure 1b

shows an example for such a deconvolution method applied to the NaPW-glass sample. This deconvolution was done for all glasses except the W free sample. Thus, the optical band gap (E_{opt}) value can be calculated using Tauc's plot by the following relation [28]:

$$\alpha h\nu = -f\,(E_{opt} - h\nu)^2 \qquad (3)$$

where $h\nu$ is the photon energy, f is constant, furthermore α is calculated from absorbance (A) and thickness (l)

$$\alpha l = 2.303(A) \quad (4)$$

The E_{opt} can be determined by extrapolating of a straight section to the value $h\nu$ =0 in x-axis in the plot of hv versus $\alpha h\nu^{1/2}$ (Fig.2 (a and b)). It is significant to observe that by increment dopants content (WO_3), the E_{opt} of NaPW- glasses get decreased. Fig. 3 displays that the estimated values of E_{opt} for NaPW- glass system. In comparison, our results are consistent with those obtained in Refs [8,29]. According to Fajan and Kreidle [30], the cations' polarizability is directly proportional to cation's positive charge and inversely proportional to cations' radius. Compared to P_2O_5, W^{6+} have a higher positive charge and a medium cation radius (0.6 Å), so W^{6+} has the highest polarizability. Moreover, the WO_3 has much smaller band gap (2.7 eV) [29] than that of P_2O_5 (8.5 eV). So, the high polarizability and small band gap of WO_3 produced the reduction in glass band gap. Further, the absorption edge in numerous materials applies the Urbach rule [28].

$$\alpha h\nu = \alpha_0\,(h\nu/E_U) \qquad (5)$$

where α_o is a constant and (E_U) is Urbach energy and refers to width of localized states tail in the forbidden band gap of the material. The exponential relation between α and

$h\nu$ may result from the electronic transitions between the localized states, which already present in the forbidden band gap [28]. Further, this exponential relation between α and $h\nu$ might arise from the random fluctuations of the internal fields related to the structural disorder in various materials. E_U is determined from the inverse slopes of ln(α) versus hν graph. As demonstrated from Fig. 3, Urbach energy (E_U) get increased by increment dopants content (WO_3). The shift towards smaller energy is associated to the creation of NBO which binds excited electrons less tightly than BO. Therefore, it might be proposed that the NBO content rises with increment WO_3 content, leading to a reduction in the values of E_{opt}. Comparable results were reported before for glasses containing WO_3 [8,29,31]. While exponential band tailing can elucidate the increasing in the amount of localization of electrons correlated to the augmentation of NBO, thereby augmenting the number of donor centers. A large amount of donor centers will efficiently decrease the band gap and shift the absorption to the smaller wavelengths.

3.2 Macro- and micro- structural parameters

The density is a macroscopic tool to recognize the microscopic variations in the material structure. It provides important information about physical and optical features. The density measurements were repeated four times the average value is listed in Table 1. It is clear that, the average density (ρ_{exp}) increases gradually from 2.49 to 3.07 g/cm^3 with WO_3 adding. This noticed increment in density is attributed to the variance between the composition content's molar weight; where the addition of a higher molecular weight rather than a lower one; (WO_3 = 231.84 g/mol.), (P_2O_5 = 141.94 g/mol.).

Table 1 offers the alteration of ρ_{exp} and V_m with WO_3 adding. It can be seen that the V_m values diminished regularly from 47.37 to 44.28 cm^3/mol, with the gradual substitute of P_2O_5 by WO_3. Such decrement may be ascribed to the succeeding points: I) The reduction in the number of oxygen ions in the glassy matrix, since five oxygen ions (P_2O_5) are substituted by three ions (WO_3). II) The reduction of the positive ions also, since two P ions are substituted by a W ion. III) The differences between the covalent radii of phosphorus (1.06A^o) and tungsten (1.3A^o) (where two phosphorus is approximately of (2.12A^o). All these reasons act to decrease the V_m of NaPW-glasses with further WO_3 addition. Another suggestion of the diminution in V_m is the simultaneous decrement of average inter – atomic separation in the glass matrix; as recorded in Table 1.

Table. 1

Indeed, a number of significant physical parameters can be estimated from the density data, such as W cation concentration, N_W (number per unit volume), Average **i**nteratomic separation in the glass matrix (r_i), polaron radius (r_p), and average field strength (F) by using equations in Ref [32] These parameters and their formulas are registered in Table 1. Where z_i is the mole fraction of WO_3, N_A is Avogadro's number, and M_W is the average molecular weight of such specimen. The W cations concentration was found to increase with WO_3. In contrast, the polaron radius and W-W Interatomic separation were found to decrease. This trend consistent with that obtained for the V_m. The average field strength was also computed and found to increase with increasing WO_3. This increment is attributed to the augmentation in electrostatic interaction due

to increasing in W concentration accompanied with decreasing in Average **i**nteratomic separation in the glass matrix.

3.3 Radiation shielding properties

For the five prepared glasses, the linear attenuation coefficient (LAC) was obtained and exhibited versus photon energy in Fig. 4. The Phy-X software was used for the determination of the LAC between 0.284 and 2.506 MeV [33]. By analyzing the figure, two main trends were noticed. First, at all photon energies, LAC decreases as energy increases for all five NaPW# glasses. This trend can be subdivided into two sections. The first energy region, region a, between 0.284 MeV and 0.826 MeV, is the energy range where the photoelectric effect is dominant. A sharp decrease in the LAC values can be observed in region a. For instance, at this low energy region, the LAC of the NaPW0 glass decreases from 0.271 to 0.172 cm^{-1} as the energy increases from 0.284 MeV to 0.826 MeV. LAC relatively decreases in a small rate at the range (1.173 MeV and 2.506 MeV). At 1.173 MeV NaPW0, NaPW5, NaPW10, NaPW15 and NaPW20 LAC becomes 0.145, 0.151, 0.162, 0.168 and 0.180 cm^{-1} respectively. This zone, (say zone b), is dominated by Compton scattering, which is behind the slower decrease in values. The significance of WO_3 percentage in the glass can be seen in the values of LAC in various samples of glasses and at any energy ranges. For example, at NaPW20, which has the richest quantity of WO_3, LAC is taking the highest value while NaPW0, which has the least quantity of WO_3 (0 mol%), LAC is taking the lowest value. For example, LAC takes the value of 0.250 cm^{-1} and 0.432 cm^{-1} for NaPW0 and NaPW20 at 0.347 MeV respectively. As seen in Fig. 4 and at higher energies, the difference between the values

largely decreases though it is maintained at all energy values. At 2.506 MeV, NaPW0 has a LAC of 0.098 cm^{-1}, while NaPW5 has a LAC of 0.120 cm^{-1}. It is clear that, the obtained results at higher energies look much closer to each other. Since a greater value of LAC indicates a better shielding capability, NaPW20 exhibits the better promising shielding properties through the NaPW# specimens at lower energy values. At higher energies, the shielding capabilities of the samples look close to each other. Then it is deducible that the amount of WO_3 in this glass sample has an important impact on the shielding capability at lower energy values and has a slight impact at higher energy values.

The (HVL) is the half value layer of the material with various percentages of WO_3 has been studied and put versus energy values in Fig.5. HVL begins with a tiny value (varied between 1.26 and 2.56 at 0.284 MeV). The HVL then experiences a rapid increase. From the Fig.5, the HVL for NaPW0 (as an example) changes from 2.56 cm (at 0.284 MeV) to 3.25 cm (at 0.511 MeV), to 4.03 cm (at 0.826 MeV) and to 7.08 cm (at 2.506 MeV). The same trend in the HVL values with the energy values is documented for the other glass samples. This behavior happens upon the increase of photons energy. Then a considerable number of photons can penetrate inside the sample material. One can deduce that, reducing the intensity of the incident photons in half requires greater thickness of the material. According to the same figure, HVL getting lower values as the WO_3 percentages increases. This phenomenon is referred to the inverse relationship, which connected density and HVL; upon the increase of WO_3 concentration, the density of the glass material increases which leads to a decrease in HVL value. Once a lower HVL indicates a more effective protector against radiation, the

figure signifies that when WO_3 getting grater content wise, the glass sample will be better as a shield against radiation.

The influence of the density of the glass samples on the shielding competence can be determined by plotting the tenth value layer (TVL) as a function of the density (see Fig.6). The TVL was determined using the formula:

$$TVL = \frac{2.3}{LAC} \qquad (3)$$

Fig.6 shows that the TVL for the glass samples declined with the increase in density, indicating that the shielding competence of the glass system can be enhanced with higher density. In addition, it was also observed that the shielding competence of the glass system was better at low energy radiation (TVL is small for 0.284 MeV). From the data provided in Fig.6, the glass samples' shielding competence were significantly improved when density was increased from 2.5 to 3.1 gcm^{-3}, as a dense medium would increase the possibility of radiation colliding with electrons in the atoms of the elements of the glass system. At a high energy level (2.506 MeV), the thicknesses of the glass required to block most of the radiation were relatively large, which were 23.509 cm, 22.489 cm, 20.784 cm, 19.980 cm, and 18.615 cm, respectively for glass samples with 0 mol% to 20 mol% of WO_3 content.

Also, we reported the mean free path (MFP) for the fabricated glasses in Fig.7. Samples with a low MFP have been found to be more useful for applications in radiation-related fields as a low MFP means a high LAC (HVL=1/LAC) [34]. Hence, more attenuation is expected for a sample with low MFP**.** The results given in Fig.7 showed that the addition of WO_3 led to an increase in density that was responsible for

the decrease in the MFP. The addition of WO_3 resulted in decreased MFP from 3.693 to 1.821 cm at 0.284 MeV, from 3.999 to 2.314 cm at 0.347 MeV, from 5.820 to 4.521 cm at 0.826 MeV and from 10.210 to 8.084 cm at 2.506 MeV. These results further emphasized the importance of density of the prepared samples in determining the sample thickness that was able to attenuate certain desired radiation levels. Additionally, we can see from Fig.7 that the energy of the photon is also affected the MFP values. The lowest values of MFP were at 0.284 MeV within the range of 1.821 to 3.693 cm. The results also revealed that at 2.506 MeV, samples had the greatest MFP compared to the other energy levels. The glasses attenuated the smallest amount of radiation at the highest energy level. This indicated that the increase in energy positively correlated with an increase in MFP and that a thicker NaPW glass is preferred for applications

The ratio between photons that passed through the NaPW glasses to the total incident radiations is called transmission factor (TF). Lower TF means more ability for the sample to serve as shielding material against radiation. The TF of NaPW0 and NaPW20 samples at four various thickness were plotted in Fig.8 and Fig.9 respectively**.** The selected thicknesses are 0.2 cm, 0.5 cm, 0.75 cm, and 1 cm, represents thinner and thicker specimens. The two figures show a decreasing behavior as the thickness increases. Also, the TF increases with increasing the energy. TF will be increased because of the ratio increase, which occur due to the increasing number of photons that penetrate through the sample at higher energies. For the sample NaPW0 with a thickness of 0.2 cm, the minimum TF value, which happens at 0.284 MeV, is equal to 94.7%, and this becomes 98.1% at 2.506 MeV. The same trend was observed for the

same glass sample at a thickness of 1 cm. The TF for this thickness at 0.284 MeV is 76.3%, and this is increased to 90.7% for a photon with energy of 2.506 MeV. For NaPW20 glass, this is also correct, namely, the TF at a specific thickness increases with increasing the energy. For instance, from Fig.9, the TF for a sample with x= 0.75 cm at 0.284, 0.511, 0.826 and 2.506 MeV are respectively 66.2%, 79.5%, 84.7% and 91.1%. The TF results also proved that the greater the thickness of the sample, the lower the TF, and the better the shielding properties. In addition, a thicker shielding material is desirable as many collisions can happen between the sample and the incident photons, attenuating the radiation. At low energy values, a big difference between thick and thin material samples can be easily noticed. Comparison between the effect of the WO_3 in each glass sample on the TF values and accordingly on the shielding properties of the prepared glasses can be examined from both Figs.8 and 9. It is found that, TF experiences a decrease with WO_3 in the sample indicating higher percentage of WO_3 has more influence in radiation attenuation purposes. At the same energy, the TF for NaPW0 (with lowest percentage of WO_3) is lower than the TF for NaPW20 (with highest percentage WO_3) for all thicknesses. These findings show that the richer the WO_3 percentage in the glass samples, the more influence the glass will be as a protection material against radiation.

Fig. 10 exhibits the effective atomic number (Z_{eff}) of the glass samples at the examined energies (i.e. between 0.284 and 2.506 MeV). Effective radiation shielding capability match up with a greater Z_{eff} since more radiation are absorbed by the medium with high Z_{eff} values. The results show a similar trend when compared to LAC values. The values are in a direct proportionality with the WO_3 content in the glass.

Instantaneously, the Z_{eff} for NaPW0 and NaPW20 glasses with 0 mol% and 20 mol% of WO_3 respectively increases from 10.02 to 18.84 at 0.284 MeV, from 10.01 to 13.56 at 0.662 MeV, and from 10.00 to 12.72 at 1.33 MeV. On the other words, at all energies, Z_{eff} goes with the trend of NaPW0 < NaPW5 < NaPW10 < NaPW15 < NaPW20. This trend in Z_{eff} emphasizes again that the greater the WO_3 percentage in the glass material, the better the shielding characteristics against radiation the glass. According to the Z_{eff} values, NaPW20 will be the most capable shielding sample among the studied glasses. Further, the radiation shielding parameters were investigated for the prepared glasses. WO_3 addition improves these shielding parameters against radiation. Where, upon the increase of WO_3 concentration, the LAC of glass material increases which leads to a decrease in HVL value. Then it is deducible that the amount of WO_3 in this glass sample has an important impact on the shielding capability at lower energy values and has a slight impact at higher energy values

4. Conclusion

We prepared a series of sodium phosphate glasses by varying WO_3/P_2O_5 content and studied structure optical and radiation shielding properties as a function of glass composition. The average density (ρ_{exp}) and was found to increase gradually from 2.49 to 3.07 g/cm^3 while the average molar volume values decreased gradually from 47.37 to 44.28 cm^3/mol with WO_3 addition. Also, the average field strength was also computed and found to increase with increasing WO_3. The study of optical absorption spectra reveals that, the absorption peaks in the visible region become higher compared to the peaks In the UV region. This observation is accompanied with a color

transformation of glasses from light to dark blue color, with more WO_3 adding. The existence of pentavalent tungsten state (W^{5+}) is identified by this blue color. with WO_3 addition an absorption band at around at 350–390 nm is appeared. Moreover, this band is overlapped with Urbach edge, which regularly produces an artificial edge-like feature at ~400 nm. A detailed deconvolution protocol is required for an appropriate understanding of these spectra and unravelling the hidden Urbach edge. The optical band gaps were determined by analyzing the optical absorption edge using the Tauc's model. Our analysis shows that, with increasing WO_3/P_2O_5 content, the absorption edge shifts toward longer wavelengths and the optical band gap decreases. This behavior can be explained in terms of lower band gap of W (2.7 eV) than that of P_2O_5 (8.5 eV) and the high polarizing power W. Further, the radiation shielding parameters were investigated for the prepared glasses. WO_3 addition improves these shielding parameters against radiation. Where, upon the increase of WO_3 concentration, the LAC of glass material increases which leads to a decrease in HVL value. Then it is deducible that the amount of WO_3 in this glass sample has an important impact on the shielding capability at lower energy values and has a slight impact at higher energy values.

Acknowledgement

This research was funded by the Deanship of Scientific Research at Princess Nourah bint Abdulrahman University through the Fast-Track Research Funding Program.

Declaration of interests

The authors declare that they have no known competing financial interests or personal relationships that could have appeared to influence the work reported in this paper.

References

1. M. R. Dousti, G. Y. Poirier, A. S. S. de Camargo, Structural and spectroscopic characteristics of Eu^{3+}-doped tungsten phosphate glasses, Optical Materials 45 (2015) 185–190.
2. A.H. Hammad, E. B. Moustafa, Study some of the structural, optical, and damping properties of phosphate glasses containing borate, Journal of Non-Crystalline Solids 544 (2020) 120209.
3. A.M. Abdelghany, Photochromic behavior of tungsten ions in sodium metaphosphate glass and effect of oxidizing condition assessed by spectroscopic analysis, Journal of Non-Crystalline Solids 552 (2021) 120460.
4. D. Möncke, Doris Ehrt–glass chemical research in the spirit of Otto Schott, Phys. Chem. Glasses Eur. J. Glass Sci. Technol. B 56 (6) (2015) 217–234.
5. D. Möncke, Photo-ionization of 3d-ions in fluoride-phosphate glasses, Int. J. Appl. Glass Sci. 6 (3) (2015) 249–267.
6. G. Poirier, F.C. Cassanjes, Y. Messaddeq, S.J. Ribeiro, Crystallization of monoclinic WO3 in tungstate fluorophosphate glasses, J. Non Cryst. Solids 355 (7) (2009) 441–446.
7. G. Poirier, F.S. Oltoboni, F.C. Cassanjes, A. Remonte, Y. Messaddeq, S.J.L. Ribeiro, Redox behavior of molybdenum and tungsten in phosphate glasses, J. Phys. Chem. (B) 112 (2008) 4481–4487.

8. G. Poirier, A. Michalowicz, Y. Messaddeq, S.J.L. Ribeiro, Local order around tungsten atoms in tungstate fluorophosphate glasses by X-ray absorption spectroscopy, J. Non-Cryst. Solids 351 (2005) 3644.

9. G. Poirier, Y. Messaddeq, S.J.L. Ribeiro, M.J. Poulain, New tungstate fluorophosphate glasses, J. Non-Cryst. Solids 351 (2005) 293.

10. S. M. Salem, Dielectric properties, conductivity, UV–visible and infrared spectroscopy of PbO-P_2O_5 NaF glasses containing WO_3, Journal of Non-Crystalline Solids 358 (2012) 1410–1416

11. Nimitha S. Prabhu, Vinod Hegde, M.I. Sayyed, E. Şakar, Sudha D. Kamath, Investigations on the physical, structural, optical and photoluminescence behavior of Er3+ ions in lithium zinc fluoroborate glass system, Infrared Phys. Technol. 98 (2019) 7–15.

12. Vinod Hegde, Nimitha Prabhu, Akshatha Wagh, M.I. Sayyed, O. Agar, Sudha D. Kamath, Influence of 1.25 MeV gamma rays on optical and luminescent features of Er3+ doped zinc bismuth borate glasses, Results in Phys. 12 (2019) 1762–1769.

13. A.E. Ersundu, M. Büyükyıldız, M. Çelikbilek Ersundu, E. Şakar, M. Kurudirek, The heavy metal oxide glasses within the WO3-MoO3-TeO2 system to investigate the shielding properties of radiation applications, Prog. Nucl. Energy 104 (2018) 280–287.

14. M.I. Sayyed, G. Lakshminarayana, M.G. Dong, M. Çelikbilek Ersundu, A.E. Ersundu, I.V. Kityk, Investigation on gamma and neutron radiation shielding parameters for BaO/SrO–Bi2O3–B2O3 glasses, Radiat. Phys. Chem. 145 (2018) 26–33.

15. H.A. Saudi, W.M. Abd-Allah, Structural, physical and radiation attenuation properties of tungsten doped zinc borate glasses, Journal of Alloys and Compounds 860 (2020) 158225.

16. H. Tekin, M. Sayyed, S.A. Issa, Gamma radiation shielding properties of the hematite-serpentine concrete blended with WO_3 and Bi2O3 micro and nano particles using MCNPX code, Radiat. Phys. Chem. 150 (2018) 95–100.

17. M.A. Marzouk, Y.M. Hamdy, H.A. ElBatal, Optical and structural properties of WO_3-doped silicophosphate glasses for gamma-ray applications, Journal of Molecular Structure 1056–1057 (2014) 227–232

18. M.A. Ouis, H.A. ElBatal, M.A. Azooz, A.M. Abdelghany, Characterization of WO_3-doped borophosphate glasses by optical, IR and ESR spectroscopic techniques before and after subjecting to gamma irradiation, Indian J. Pure and Appl. Phys. 51(2013) 11.

19. Y. Mei, W.C. Zheng, Spin-Hamiltonian parameters and tetragonal distortion for the (WO_6) 7– octahedral centers in the WO_3-doped Zn $(PO_4)_2$ ZnO nanopowders, Optik 179 (2019) 965–968.

20. D. Möncke, D. Ehrt, Photoinduced redox-reactions and transmission changes in glasses doped with 4d-and 5d-ions, J. Non. Cryst. Solids 352 (2006) 2631–2636.

21. D. Möncke, D. Ehrt, Photoinduced redox reactions in Zr, Nb, Ta, Mo, and W doped glasses, Phys. Chem. Glasses-Eur. J. Glass Sci. Technol. Part B 48 (5) (2007) 317–323.

22. M.A. Ouis, M.A. Azooz, H.A. ElBatal, Optical and infrared spectral investigations of cadmium zinc phosphate glasses doped with WO3 or MoO3 before and after subjecting to gamma irradiation, Journal of Non-Crystalline Solids 494 (2018) 31–39.

23. A. Knowles, C. Burgess, Practical Absorption Spectrometry: Ultraviolet Spectrometry Group, Springer Netherlands, Dordrecht, 1984.

24. Faten Al-Hazmi, S.F. Mansour, M.S. AlHammad, M.A. Abdo, M.S. Sadeq, Impact of sunlight on the optical properties and ligand field parameters of nickel borosilicate glasses, Ceram int, (in press).

25. S. B. Mallur, T. Czarnecki, A. Adhikari, P. K. Babu. "Compositional dependence of optical band gap and refractive index in lead and bismuth borate glasses", Materials Research Bulletin 68 (2015) 27–34

26. S. Kasap, P. Capper. Springer handbook of electronic and photonic materials. USA: Springer; (2006) 58.

27. M.S. Sadeq, H.Y. Morshidy. Effect of mixed rare-earth ions on the structural and optical properties of some borate glasses. Ceram Int. 45 (2019) 18327.

28. Tauc, R. Grigorovici, A. Vancu, Optical properties and electronic structure of amorphous germanium, Phys. Status Solidi B 15 (1966) 627–637.

29. Q. Chen, WO_3 concentration-dependent magneto-optical properties of Faraday rotating glasses and glass-ceramics, Journal of Non-Crystalline Solids 522 (2019) 119584.

30. J.A. Duffy, Optical basicity: a practical acid–base theory for oxides and oxyanions, J. Chem. Educ. 73 (12) (1996) 1138–1142.

31. Shaaban M. Salem, E.K. Abdel-Khalek, E.A. Mohamed, M. Farouk, A study on the optical, structural, electrical conductivity and dielectric properties of a lithium bismuth germanium tungsten glasses, J Alloys Compd 513 (2012) 35–43.

32. M.S. Sadeq, M.A. Abdo, Effect of iron oxide on the structural and optical properties of alumino-borate glasses, Ceram. Int., 47 (2021) 2043–2049

33. Erdem Şakar, Özgür Fırat Özpolat, Bünyamin Alım, M.I. Sayyed, Murat Kurudirek, Phy-X / PSD: Development of a user-friendly online software for calculation of parameters relevant to radiation shielding and dosimetry, Radiation Physics and Chemistry 166 (2020) 108496

34. Y. Al-Hadeethi, M.I. Sayyed, $BaO–Li_2O–B_2O_3$ glass systems: Potential utilization in gamma radiation protection, Progress in Nuclear Energy 129 (2020) 103511

Figures

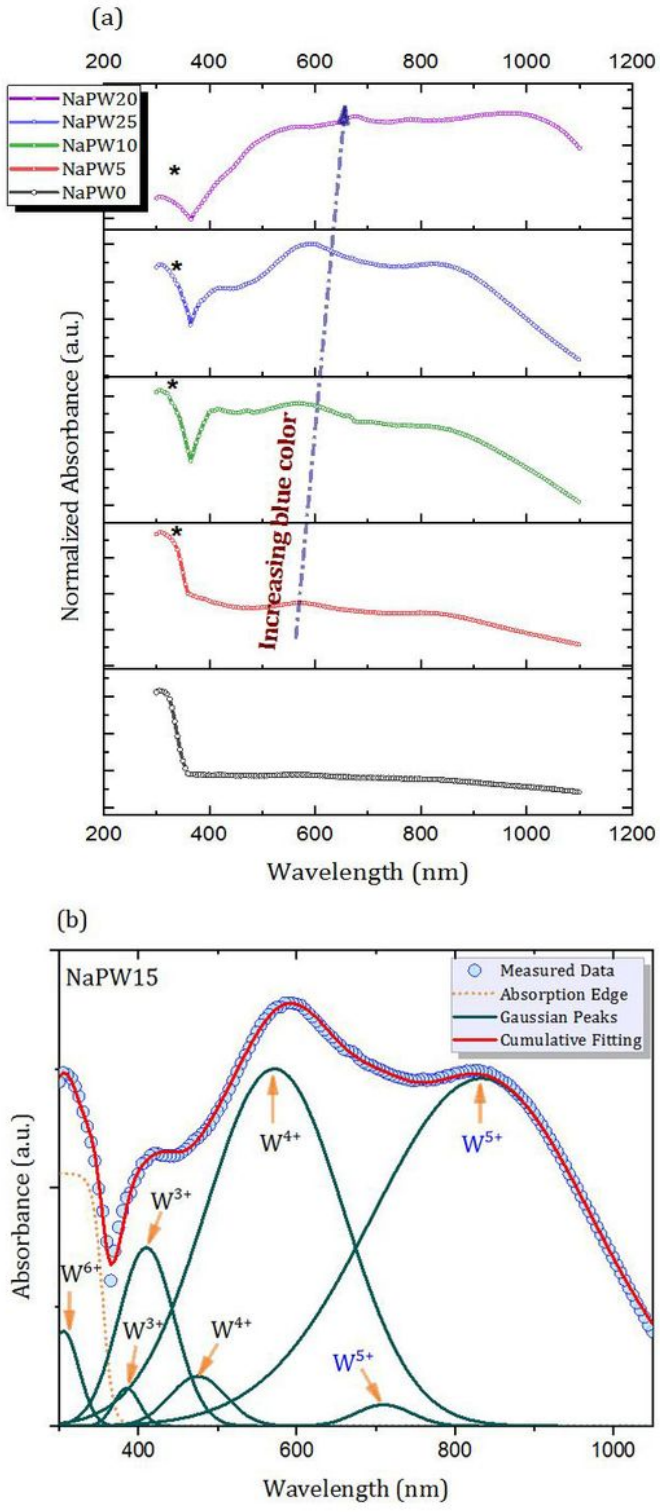

Figure 1

a. Optical absorption spectra as a function of wavelength for the prepared glass samples. b. The deconvoluted optical absorption spectra for the sample that contains 15% WO3 as a representative figure.

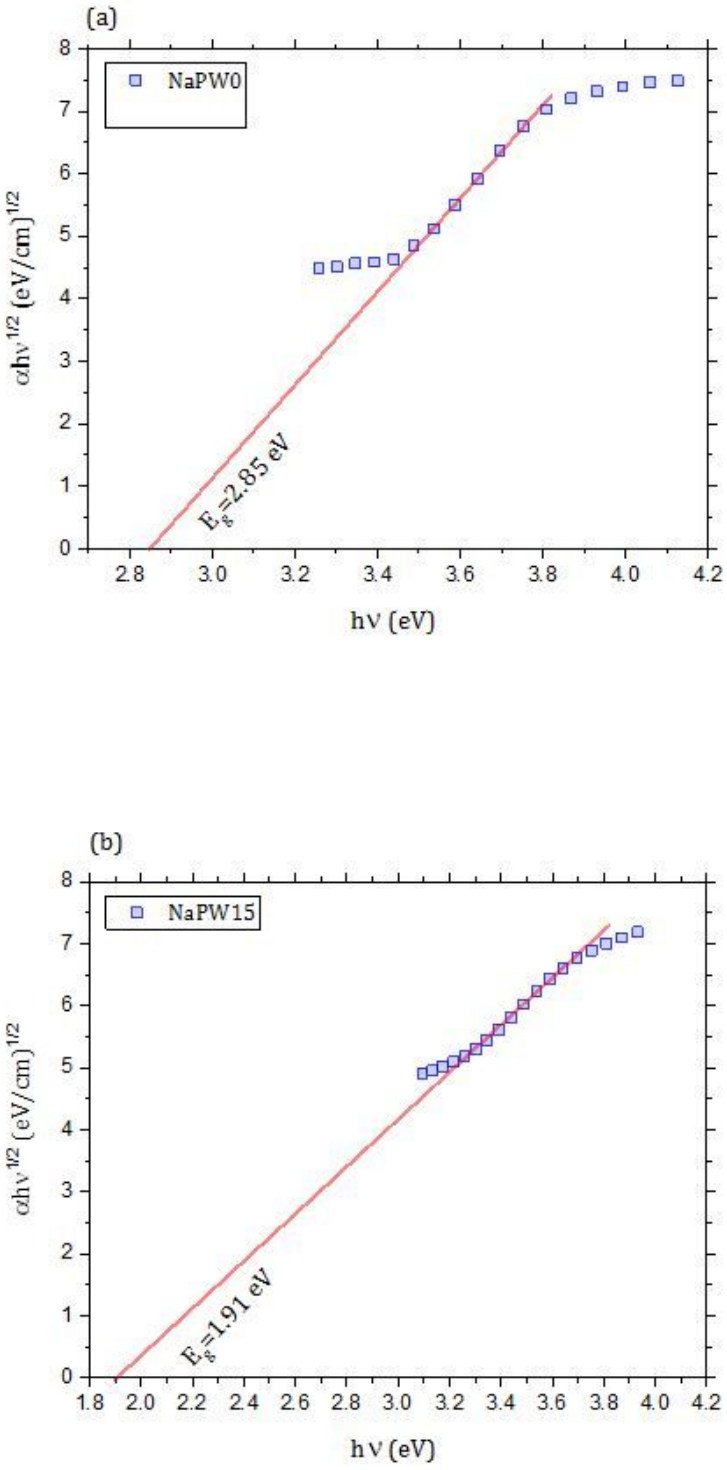

Figure 2

a. The change of ahn1/2 versus hn (for indirect transitions) for the sample that contains 0% WO3. b. The change of ahn1/2 versus hn (for indirect transitions) for the sample that contains 15% WO3.

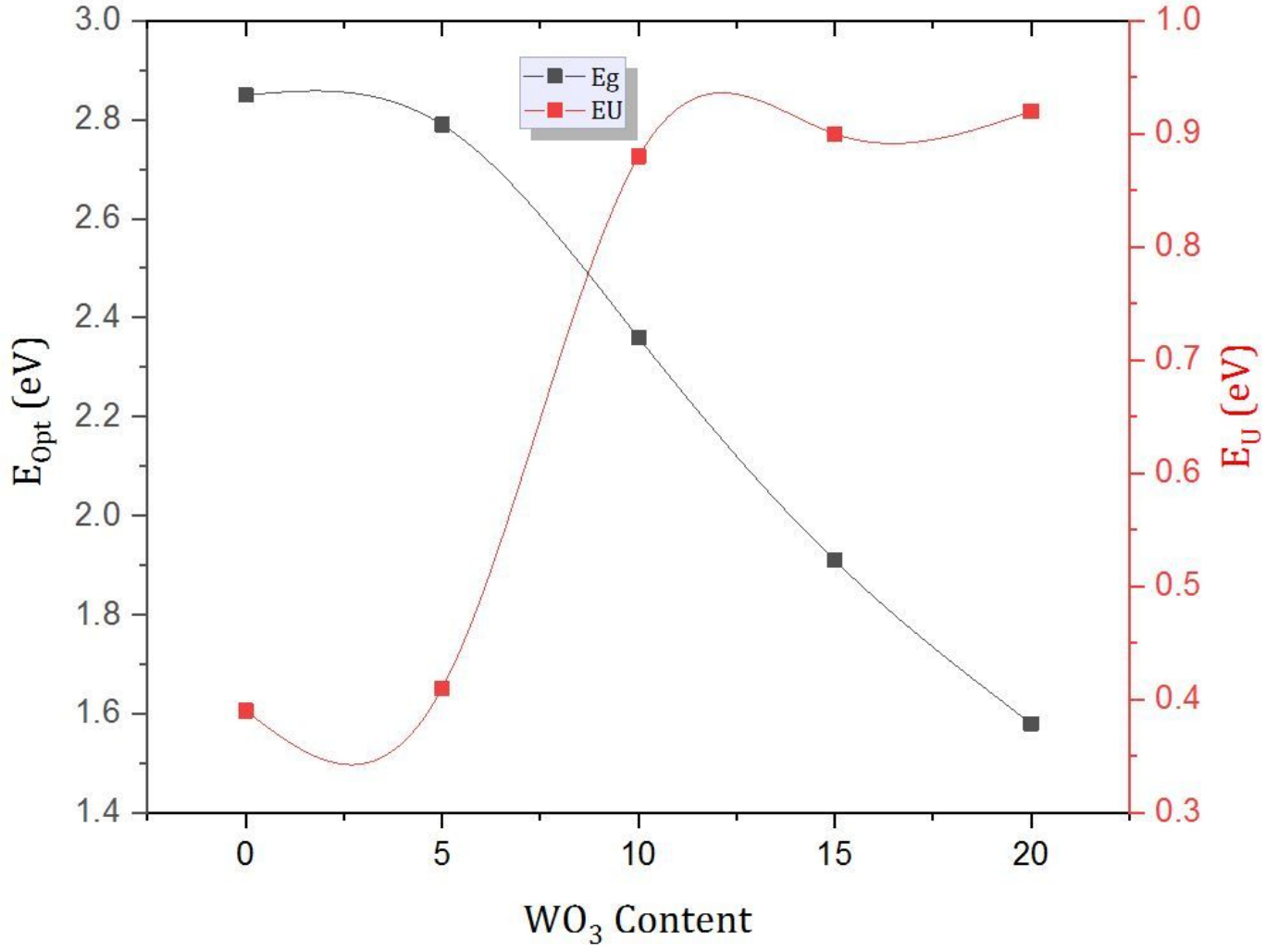

Figure 3

The change of Eopt and versus WO3 content for the prepared glass samples.

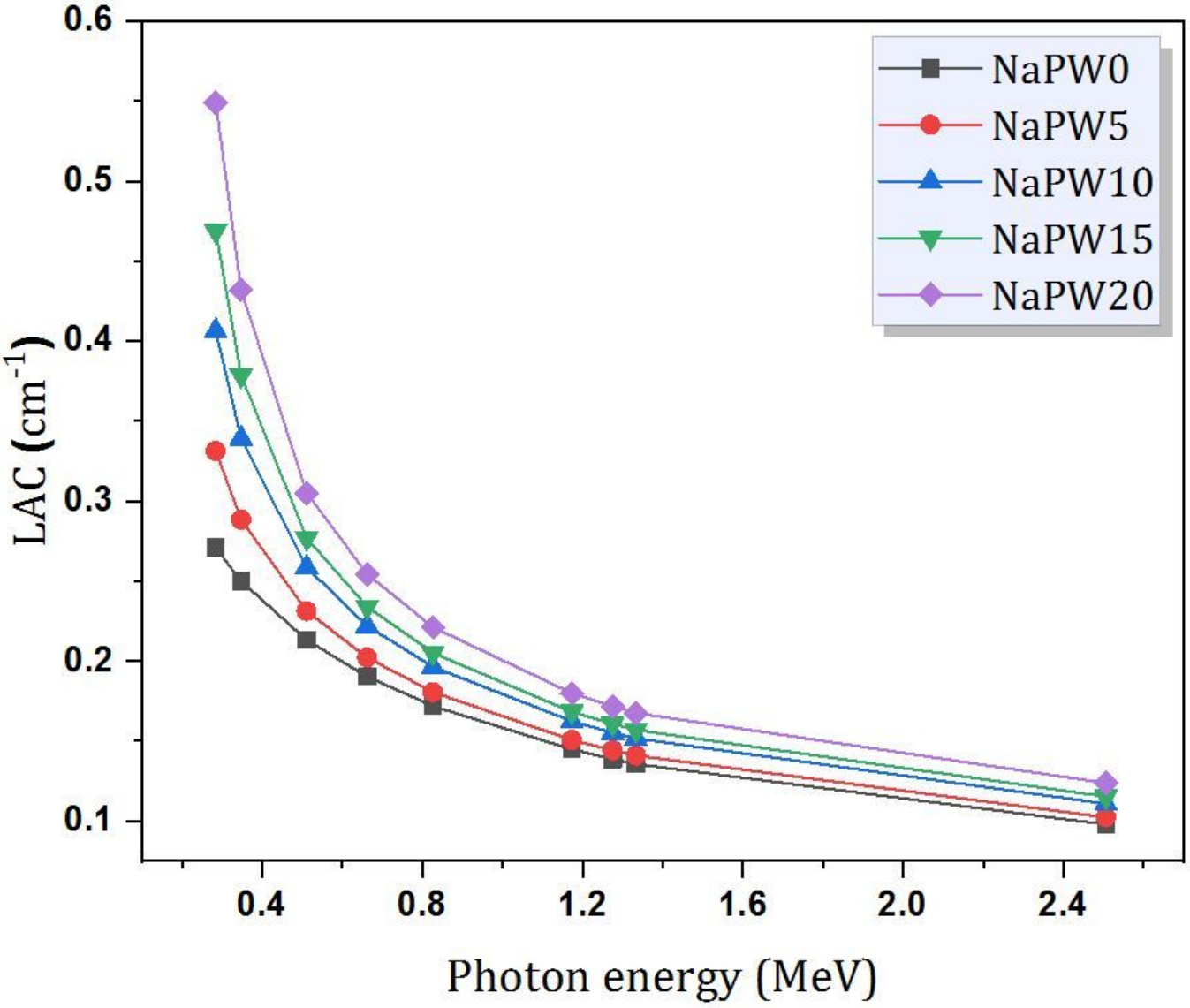

Figure 4

The linear attenuation coefficient as a function of the energy for the prepared glasses

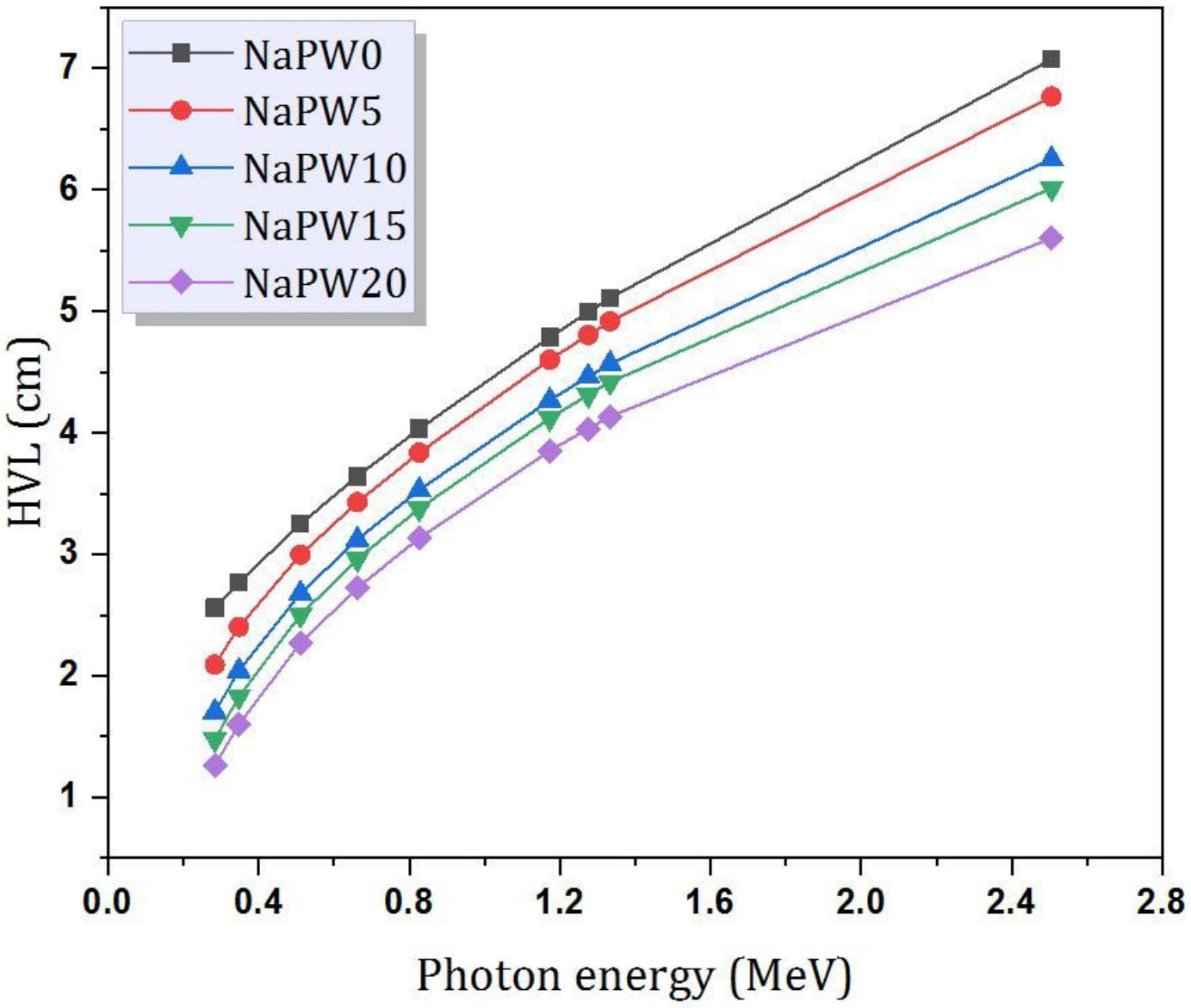

Figure 5

The half value layer as a function of the energy for the prepared glasses

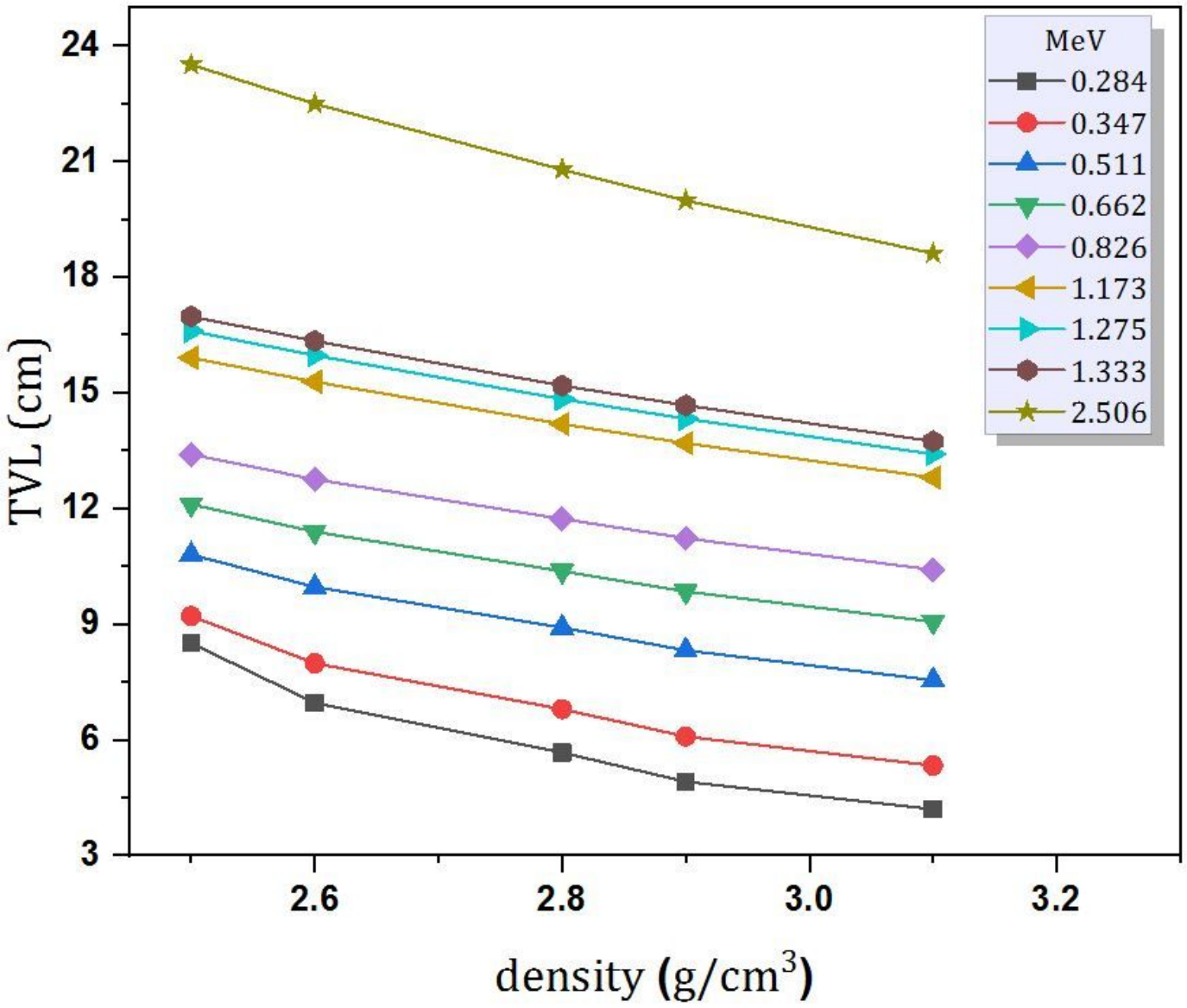

Figure 6

The tenth value layer as a function of the density for the prepared glasses

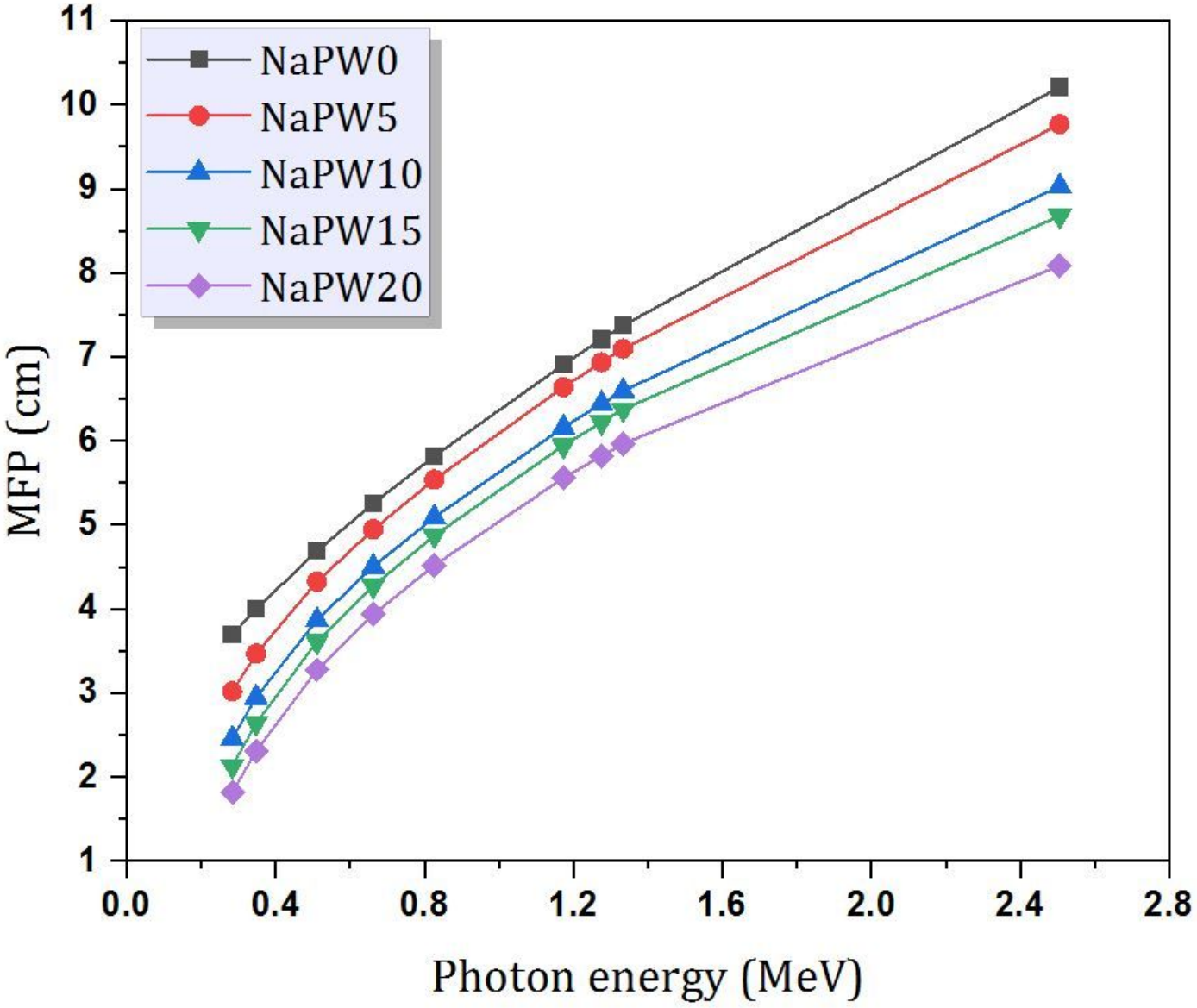

Figure 7

The mean free path as a function of the energy for the prepared glasses

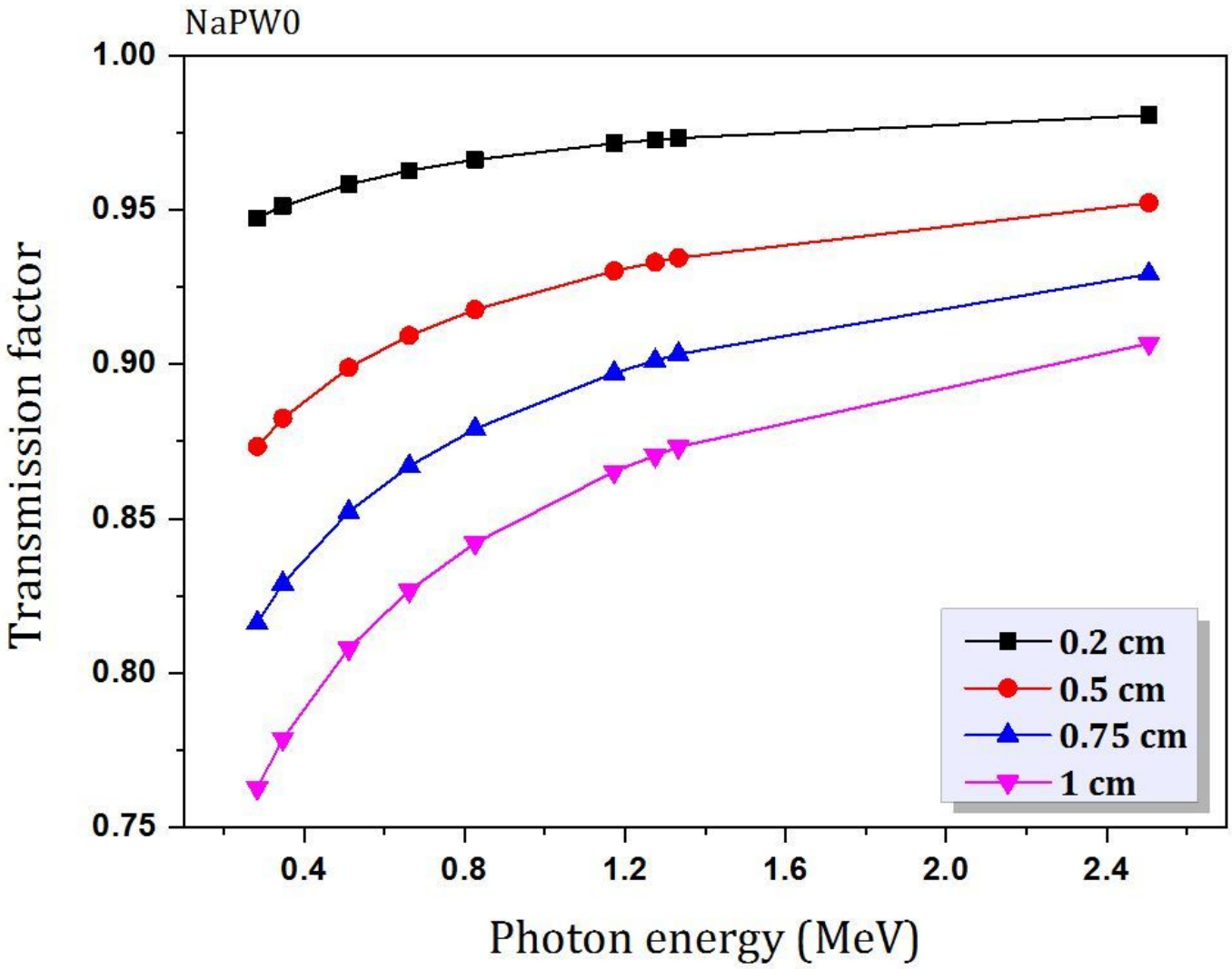

Figure 8

The transmission factor as a function of the energy for the NaPW0 glass

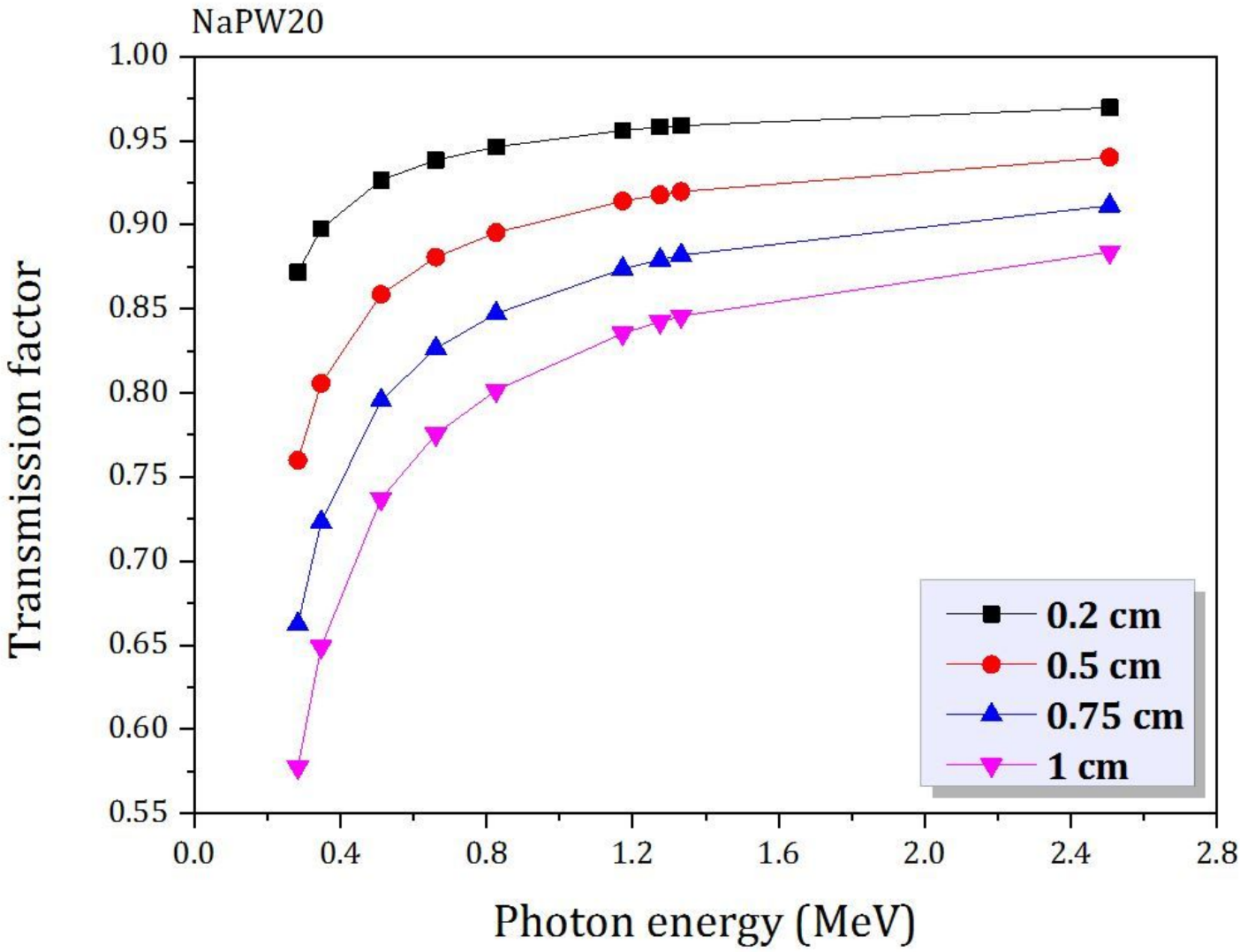

Figure 9

The transmission factor as a function of the energy for the NaPW20 glass

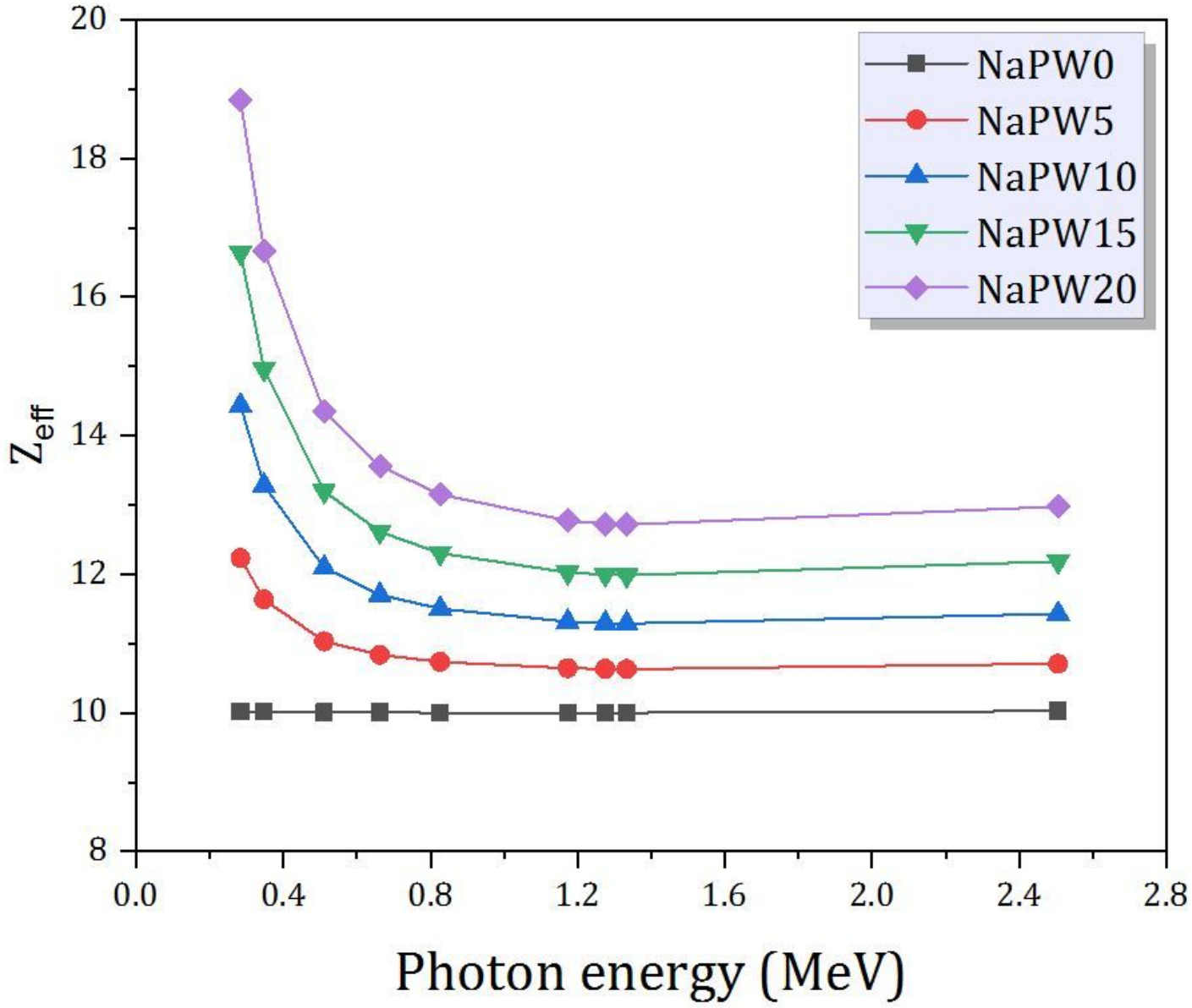

Figure 10

The effective atomic number as a function of the energy for the prepared glasses